

K⁺ p ELASTIC SCATTERING AT 3.0 GeV/c

J. Debaisieux, F. Grand, J. Heughebaert, L. Pape and R. Windmolders,
Laboratoire des Hautes Energies, Bruxelles

R. George, Y. Goldschmidt-Clermont, V.P. Henri, D.W.G. Leith,
G.R. Lynch, F. Muller and J.-M. Perreau,
CERN, Geneva

G. Otter* and P. Sällström,
Institute of Physics, Stockholm.

Abstract

In the course of a systematic study of K⁺p interactions at 3.0 GeV/c, the elastic scattering reaction has been investigated. A total of 1720 events were identified as elastic scatters, giving a cross-section of $(4.8 \pm .4)$ mb. The angular distribution shows characteristic diffraction peaking and was fitted using

$$\frac{d\sigma}{d|t|} = \left(\frac{d\sigma}{d|t|}\right)_0 e^{\alpha t + \beta t^2},$$

in the momentum transfer region $(0.05 - 1.14)$ (GeV/c)². The best fit gave $\alpha = 4.55 \pm 0.39$ (GeV/c)⁻² and $\beta = 0.64 \pm 0.42$ (GeV/c)⁻⁴. The extrapolated experimental cross-section at 0⁰, $(d\sigma/dt)_0$, is found to be (19.5 ± 2.3) mb/(GeV/c)², and exceeds the optical theorem prediction by (3.8 ± 2.3) mb/(GeV/c)², implying that there is a contribution from the real part of the K⁺p scattering amplitude at 3.0 GeV/c.

Introduction

The elastic scattering of K⁺ mesons on protons has been studied up to 2.0 GeV/c using emulsion, bubble chamber and counter techniques. From the data of Cook et al.⁽¹⁾, and later Chinowsky et al.⁽²⁾, it appears that at 1.97 GeV/c the distribution of the centre of mass scattering angle of the K⁺ is strongly peaked in the forward direction. The same effect was found by Foley et al.⁽³⁾ in the region 7 - 15 GeV/c. No results have been published between 2 - 7 GeV/c.

* Now at Institut für Theoretische Physik, Vienna, Austria

+ Now at Lawrence Radiation Laboratory, Berkeley, California

This report presents data obtained in an analysis of K^+p elastic scattering at 3.0 GeV/c and represents the first part of a study of K^+p interactions at 3.0, 3.5 and 5.0 GeV/c. Preliminary results have been presented at the Dubna Conference, 1964⁽⁴⁾.

Experimental Details

The Saclay 80 cm hydrogen bubble chamber was exposed to a separated beam of K^+ (5) mesons at the CERN proton-synchrotron. The momentum of the beam was determined by measurement of τ -decays and was found to be 2.97 GeV/c at the centre of the chamber, with a momentum spread of ± 0.015 GeV/c. The pion contamination was, on the average, not more than 5%.

A total of about 40,000 pictures were scanned for all two-prong events occurring within a reduced fiducial volume chosen in order to minimise measurement errors. At scanning, events which were obviously inelastic, as recognized from the momenta of outgoing tracks, were rejected. The selected events were measured and processed through the CERN programs THRESH, GRIND and BAKE. An event was accepted as elastic if the χ^2 was less than 20 for an elastic hypothesis compatible with the observed bubble densities. After remeasurements, a total of 1720 elastic events were identified. Their missing mass distribution and χ^2 distribution are shown in Figs. 1 and 2, respectively.

Those events fitting and identified as the reaction $K^+p \rightarrow K^+p\pi^0$, have been shown in Fig. 1 as the darkened area. A good separation of the elastic events is obtained on the basis of missing mass alone (the contamination under the "elastic peak" being $\approx 3\%$). However, when one applies all the available kinematic constraints, no event is found to fit simultaneously this reaction and the elastic hypothesis.

The scanning efficiency has been estimated from a second scan performed on about half of the analyzed pictures and was found to be 96% for events with $\cos \theta$ (where θ is the centre of mass scattering angle) less than 0.98, corresponding to a recoil proton range of 1.7 cm. It appeared that the scanning efficiency deteriorated rapidly for larger values of $\cos \theta$ and it was therefore decided to keep for further analysis only those events with $\cos \theta$ less than 0.98. The dependence of the scanning efficiency versus the dip angle, λ , has been studied for $\cos \theta \leq 0.98$. The dip angle, λ , is defined as the angle between the plane of

the chamber window and the scattering plane (for small scattering angles it is essentially the angle between the recoil proton and the window). The distribution of λ is shown in Fig. 3 for all identified events with $\cos \theta \leq 0.98$. It appears to be compatible with isotropy in the region $0^\circ - 60^\circ$. We made a general cut-off in λ at 80° because the configuration of the track for events with $\lambda \geq 80^\circ$ makes the geometrical reconstruction more difficult and less accurate. The fall-off in the region $60^\circ \leq \lambda \leq 80^\circ$ is found to result from events emitted at small scattering angle, and thus for $0.95 \leq \cos \theta \leq 0.98$, a cut-off was set at the value $\lambda = 60^\circ$.

Results and Discussion

(a) Cross-section

The K^+p total elastic cross-section, σ_{el} , has been determined from the number of elastic events, corrected for scanning efficiency and for the λ and $\cos \theta$ cut-off's, and from the number of τ -decays occurring in the fiducial volume considered in this experiment. Using the following values :

$(1.229 \pm 0.008) \times 10^{-8}$ sec. for the K^+ lifetime⁽⁶⁾,

(0.055 ± 0.001) for the branching ratio for K^+ decay into three charged pions⁽⁶⁾,

0.062 g/cm^3 for the density of liquid hydrogen in the bubble chamber :

the elastic cross-section has been found to be :

$$\sigma_{el} = (4.8 \pm 0.4) \text{ mb.}$$

A summary of the dependence of the elastic cross-section^{(1),(2),(3),(7)} versus the incident K^+ momentum is shown in Fig. 4, together with the K^+p total cross-section^{(2),(7),(8),(11)}. It may be expected from the rapid increase of the inelastic cross-section at about 2 GeV/c (i.e. shown by the difference between total and elastic cross-sections in Fig. 4), that the elastic differential cross-section should begin to show diffraction type behaviour above this energy. The present results do in fact demonstrate this trend.

(b) Differential Cross-section

The experimental angular distribution corrected for the imposed angular cut-offs, is represented as a function of $\cos \theta$ or $-t$ (momentum transfer squared) on Fig. 5. The values are given in Table I.

The experimental angular distribution has been fitted to the following function :

$$\frac{d\sigma}{d|t|} = \left(\frac{d\sigma}{d|t|}\right)_0 e^{\alpha t} \quad (1)$$

where α represents the slope of the distribution and $\left(\frac{d\sigma}{d|t|}\right)_0$ is the value of the cross-section at $t=0$. The fit has been made using the maximum likelihood method. The probability element is :

$$P(t) dt = \frac{e^{\alpha t} dt}{\int_{t_0}^{t_1} e^{\alpha t} dt} \quad (2)$$

where t_0 and t_1 are, respectively, the lower and upper limits between which the angular distribution is considered. The likelihood function is then

$$L(\alpha) = \prod_{i=1}^n \left[P(t_i) \right] \quad (3)$$

where the product runs over the total number of selected events (n). The best value of α is obtained when $\text{Log } L(\alpha)$ reaches its maximum value and the error $\Delta\alpha$ is given by :

$$\Delta\alpha = \sqrt{-\frac{\delta^2}{\delta\alpha^2} \text{Log } L(\alpha)}^{-1/2}, \quad (4)$$

for a gaussianly distributed $L(\alpha)$. The maximum likelihood fit was performed using the MALIK program⁽⁹⁾.

The results of the fit are given in Table II, for two different "t" intervals, together with the corresponding forward differential cross-section.

It may be seen from Table II that the slope α is found to be steeper if a small range of $\cos \theta$ is used. In fact, results obtained from fits made by taking $\cos \theta$ intervals of intermediate range between solutions I and II showed that the coefficient α varies linearly, between the two values quoted in Table II, within the limits of the estimated errors. The fact that the value of α seems to vary monotonically throughout the region of the angular distribution investigated, suggests that the experimental data would be better represented by an exponential with a quadratic term in t

$$\frac{d\sigma}{d|t|} = \left(\frac{d\sigma}{d|t|}\right)_0 e^{\alpha t + \beta t^2} \quad (5).$$

A maximum likelihood fit to the data has been made for two "t" intervals, and the results are presented in Table III⁽¹⁰⁾.

At 2.0 GeV/c, Cook et al. and Chinowsky et al. found that their differential cross-section could be adequately described by an exponential of the type $\frac{d\sigma}{d|t|} = \left(\frac{d\sigma}{d|t|}\right)_0 e^{\alpha t}$ (i.e. $\beta = 0$); however, the data of Foley et al. in the region (7 - 15) GeV/c required a term in βt^2 , as described above for this experiment. These experiments have been analysed in the "t" range up to about $1(\text{GeV}/c)^2$. The parameters shown in Tables II and III lie between the result of Chinowsky et al. at 1.97 GeV/c (viz. $\alpha = 2.9 \pm .14$), and Foley et al. at 7.0 GeV/c (viz. $\alpha = 6.2 \pm 0.9$). This verifies the rapid shrinking in the K^+p diffraction peak between 2 and 7 GeV/c, which may be interpreted as reflecting the rapid change of the inelastic cross-section at these energies⁽⁴⁾.

(c) Comparison with the Optical Point

The results of the differential cross-section in the forward direction given in Tables II and III may be compared to the prediction of the optical theorem. Taking the value of the total cross-section at 3.0 GeV/c :

$$\sigma_{\text{tot}} = (17.51 \pm 0.27) \text{ mb}$$

found by Baker et al.⁽¹¹⁾, the optical theorem point cross-section is :

$$\left(\frac{d\sigma}{d|t|}\right)_{\text{opt}} = (15.7 \pm 0.4) \frac{\text{mb}}{(\text{GeV}/c)^2}.$$

The forward scattering cross-section, as determined by this experiment, is larger than would be predicted if the scattering amplitude were purely imaginary. In fact, choosing the two-parameter fit (i.e. the best parameterisation), the following results are obtained :

$$\begin{aligned} \left| \frac{\text{Re } A}{\text{Im } A} \right| &= 0.49 \pm 0.31 \text{ for } |t| \lesssim 1.1 (\text{GeV}/c)^2 \text{ (i.e. Sol. II, Table III)} \\ &= 0.52 \pm 0.25 \text{ for } |t| \lesssim 1.8 (\text{GeV}/c)^2 \text{ (i.e. Sol. I, Table III)}. \end{aligned}$$

The data indicate that, at the 90% confidence level, there is some real part to the K^+p scattering at 3.0 GeV/c. The relative magnitude of the real and imaginary parts is poorly determined in this experiment but it is clearly compatible with the results of Foley et al.⁽³⁾, where at higher momenta (7 - 15 GeV/c), a contribution of as much as 20% from the real part of the amplitude, could not be excluded.

(d) Comparison with Optical Model Theories

Recently, Simmons⁽¹²⁾ has attempted to fit the π^{\pm} p elastic scattering data at 2.0 GeV/c, assuming a model in which all partial waves with angular momentum, l , less than a cut-off, L , are equally absorbed and that all other waves do not interact. This attempt was justified in view of the appearance of a secondary diffraction peak in the π^{\pm} p scattering data. Here no such secondary peak is present (Fig. 4) but it is still of interest to interpret our results in terms of this model due to its success in explaining π^{\pm} p⁽¹³⁾,⁽¹⁴⁾ and K^- p⁽¹⁴⁾ scattering in our energy region.

This model corresponds to the scattering by a grey disc of radius $R = \frac{L}{k}$ where k represents the wave number of the incident K^+ . The total and elastic cross-sections are given by :

$$\begin{aligned} \sigma_{\text{tot}} &= \frac{2\pi\alpha}{k^2} \cdot (L + 1)^2 \\ \sigma_{\text{el}} &= \frac{\pi\alpha^2}{k^2} \cdot (L + 1)^2 \end{aligned} \quad (6)$$

and the angular distribution is described by

$$\frac{d\sigma}{d\Omega} = \left(\frac{d\sigma}{d\Omega} \right)_0 \left[\frac{P'_L(\cos \theta) + P'_{L+1}(\cos \theta)}{(L + 1)^2} \right]^2 \quad (7)$$

where $\left(\frac{d\sigma}{d\Omega} \right)_0 = \frac{\alpha^2 (L+1)^4}{4k^2}$, $P'_L(\cos \theta)$ and $P'_{L+1}(\cos \theta)$ are the Associated Legendre Polynomials, and α is the absorption coefficient. Such a fitting to our data, for $L = 3$ (the value derived from the measured σ_{tot} , σ_{el} and the solution of equations (6)) is shown in Fig. 6. This choice of L corresponds to the scattering from a disc of radius⁽¹⁴⁾, $R \approx 0.55$ f. The absorption coefficient, α , in this case would be ≈ 0.6 . For values of $\cos \theta$ greater than 0.7 (i.e. for $-t \lesssim 0.7$ (GeV/c)²), the fit is fair, but as an overall fitting to the angular distribution this description is hardly adequate.

We also compared our data with the dependence suggested by Minami⁽¹⁶⁾ for K^+ p scattering

$$f(\theta) = i \left(\frac{1}{\sqrt{\pi}} \right) \exp \frac{1}{2} (A_0 + A_1 t) + C \quad (8)$$

where $f(\theta)$ is the elastic scattering amplitude, and A_0 and A_1 are taken to be independent of energy.

The data at 3.0 GeV/c are not in good overall agreement with such a parameterisation in which A_0 and A_1 are taken from Minami's analysis of the high energy data⁽³⁾, and C is optimised for our experiment. However, the fit is good for momentum transfers smaller than 1 (GeV/c)² (see Fig. 6), the region in which the A's were determined.

Conclusion

It has been shown above that the differential cross-section for the reaction $K^+ p \rightarrow K^+ p$ at 3.0 GeV/c is dominated by a sharp forward scattering peak. The fall-off with momentum transfer of this peak may be well represented by an exponential of the form $Ae^{\alpha t + \beta t^2}$, where β is found to be a rather small correction ($\sim 15\%$ of α around $-t=1$ (GeV/c)²). The elastic scattering cross-section is found to be in good agreement with data from neighbouring momenta, and confirms the rapid decrease in the cross-section implied by the previous data. The values of the parameters α and β are found to lie between the values found at 2.0 and 7 GeV/c, and demonstrate the rapid change of the angular distribution in this region. This effect may be interpreted as reflecting the rapid change in the inelastic cross-section over this same momentum interval. Although the angular distribution has a shape which is typical of a diffraction scattering distribution, the detailed shape cannot be satisfactorily explained by a simple two-parameter optical model theory. No evidence for the existence of secondary diffraction peaks in $K^+ p$ scattering at this energy is observed. Finally, it is also shown that the data indicate the presence of some real part in the scattering amplitude, but do not allow a good determination of the ratio $\left| \frac{\text{Re} A}{\text{Im} A} \right|$; the results obtained show $\left| \frac{\text{Re} A}{\text{Im} A} \right| \sim 0.5 \pm 0.3$, the result being fairly independent of the "t" range used in the fit.

Acknowledgments

The Belgian group is grateful to Dr. J. Reignier for helpful discussion, and the Institut Royal Météorologique de Belgique, especially to Mr. J. Van Isacker, for his help in the use of the IBM 7040 computer. They would like to thank Professor L. Rosenfeld for his support and interest.

The Stockholm group acknowledges support from the Swedish Atomic Research Council. The research reported in this paper has been sponsored in part by the United States Air Force under Grant Nos. 63-11 and 64-57, European Office of Aerospace Research.

Our thanks are due to the crew of the 81cm Saclay hydrogen bubble chamber, to the staff of the CERN proton-synchrotron, to the computing division, and to our scanning and measuring staff. We are grateful to Professor R. Armenteros for helpful discussion, and to Professor Ch. Peyrou for his support.

References

- (1) V. Cook, D. Keefe, L.T. Kerth, P.G. Murphy, W.A. Wenzel, T.F. Zipf, Phys.Rev. 129, 2743 (1963).
- (2) W. Chinowsky, G. Goldhaber, S. Goldhaber, T. O'Halloran and B. Schwangschild, U.C.R.L. 11669 (unpublished).
- (3) K.J. Foley, S.J. Lindenbaum, W.A. Love, S. Ozaki, J.J. Russell and L.C.L. Yuan, Phys.Rev.Letters 11, 503 (1963).
- (4) J. Debaisieux, F. Grard, J. Heughebaert, L. Pape, R. Windmolders, M. Ferro-Luzzi, R. George, Y. Goldschmidt-Clermont, V.P. Henri, B. Jongejans, D.W.G. Leith, G.R. Lynch, F. Muller, J.-M. Perreau, G. Otter and P. Sällström, Dubna Conference on Elementary Particles, 1964.
- (5) J. Goldberg and J. M. Perreau, CERN 63-12 (1963).
- (6) A.H. Rosenfeld, A. Barbaro-Galtieri, W.M. Barkas, P.L. Bastien, J. King and M. Roos, U.C.R.L. 8030 (revised 1965)
- (7) T. Stubbs, M. Bradner, W. Chinowsky, G. Goldhaber, S. Goldhaber, W. Slater, D. Stork and M. Ticho, Phys.Rev.Letters 7, 188 (1961),
- S. Goldhaber, W. Chinowsky, G. Goldhaber, W. Lee, T. O'Halloran, T. Stubbs, G.M. Pjerrou, D. Stork and H. Ticho, Phys.Rev.Letters 9, 135 (1962).
- (8) V. Cook, D. Keefe, L.T. Kerth, P.G. Murphy, W.A. Wenzel and T. Zipf, Phys.Rev.Letters 7, 182 (1961),

W.F. Baker, R.L. Cool, E.W. Jenkins, T.F. Kycia, R.H. Phillips and A.L. Read, Phys.Rev. 129, 2285 (1963),

W. Galbraith, E.W. Jenkins, T.F. Kycia, B.A. Leontic, R.H. Phillips and A.L. Read, Phys.Rev. 138, B913 (1965).

- (9) F. Grard, Nuclear Instruments and Methods 34, 242 (1965).

The maximum likelihood was performed on a distribution divided into small intervals of $\cos \theta$ and not on an event by event basis. However, the intervals were chosen small enough such that the results were practically independent of bin size.

- (10) Pion Contamination :

At an incident momentum of 3 GeV/c and for centre of mass scattering angles less than 90° , K^+p and π^+p elastic scattering events are undistinguishable from the point of view of kinematics and ionisation. The sample of selected K^+p events therefore may contain a contamination of π^+p elastic events. In order to evaluate the influence of this pion contamination on the shape of the experimental angular distribution, the parameters α and β have been re-evaluated assuming a 5% contamination of the beam, and using the π^+p data of Perl et al. at 2.92 GeV/c (loc.cit.). This investigation

showed a systematic tendency for the parameters to decrease but never exceeding the assigned errors. Typically, the parameters for Solution I in Table III became $\alpha = 4.44 \pm 0.26 \text{ (GeV/c)}^{-2}$ and $\beta = 0.64 \pm 0.21 \text{ (GeV/c)}^{-4}$. Since 5% is an upper limit for the contamination, we regard the effect of the pion background on the K^+ angular distribution as negligible.

- (11) W.F. Baker, E.W. Jenkins, T.F. Kycia, R.H. Phillips, A.L. Read, K.F. Riley and H. Ruderman, Sienna Conference on Elementary Particles, p.634, 1963.
- (12) L.M. Simmons, Phys.Rev.Letters 12, 229 (1964).
- (13) M.L. Perl, L.W. Jones and C.C. Ting, Phys.Rev. 132, 1252 (1963).
- (14) This radius is not the radius ordinarily quoted for diffraction on a disc: $R = \sqrt{2\alpha} \approx 0.7$ fermi, a formula which is strictly valid only at very high energy.
- (15) D.E. Damouth, L.W. Jones and M.L. Perl, Phys.Rev.Letters 11, 287 (1963),
and
R. Crittenden, H.J. Martin, W. Kernan, L. Leipuner, A.C. Li, F. Ayer, L. Marshall and M.L. Stevenson, Phys.Rev.Letters 12, 429 (1964).
- (16) S. Minami, Phys.Rev. 135, 1263 (1964).

TABLE I

Experimental angular distribution of K^+p elastic scattering at 2.97 GeV/c.

In column 2, $-t$ represents the value of the momentum transfer squared at the middle of the $\cos \theta$ interval. The numbers of events are given for dip angles ranging from 0 to 80° . The numbers corresponding to the first $\cos \theta$ interval have been obtained after a correction was made for loss of events with large dip values (see text). No mention has been made of $\cos \theta$ intervals in which no event was recorded.

cos θ interval	(Momentum transfer) ² (GeV/c) ² $-t$	Number of events	Number of events corrected	$\frac{d\sigma}{d t }$ (mb/(GeV/c) ²)
0.98 - .95	0.080	383	718	14.65 ± 1.51
.95 - .90	0.171	391	440	8.98 ± 0.91
.90 - .85	0.287	261	294	6.00 ± 0.65
.85 - .80	0.401	155	174	3.55 ± 0.43
.80 - .75	0.516	101	114	2.32 ± 0.31
.75 - .70	0.630	63	71	1.45 ± 0.23
.70 - .65	0.745	56	63	1.29 ± 0.21
.65 - .60	0.860	27	30.4	0.62 ± 0.13
.60 - .55	0.974	21	23.6	0.48 ± 0.12
.55 - .50	1.089	8	9.0	} 0.19 ± 0.04
.50 - .45	1.203	9	10.1	
.45 - .40	1.318	7	7.9	
.40 - .35	1.433	6	6.8	} 0.04 ± 0.01
.35 - .30	1.547	4	4.5	
.30 - .25	1.657	1	1.1	
.25 - .20	1.772	2	2.3	
.20 - .15	1.886	1	1.1	
.15 - .10	2.000	1	1.1	} 0.01 ± 0.01
0.0 - -0.05	2.343	1	1.1	
-0.05 - -0.10	2.457	2	2.3	
-0.10 - -0.15	2.572	2	2.3	
-0.20 - -0.25	2.800	3	3.4	
-0.30 - -0.35	3.029	1	1.1	
-0.50 - -0.55	3.486	1	1.1	
-0.75 - -0.80	4.058	1	1.1	
-0.90 - -0.95	4.401	1	1.1	
-0.95 - -1.00	4.515	1	1.1	

TABLE II

Parameters for the fit of the form $\frac{d\sigma}{d|t|} = \left(\frac{d\sigma}{d|t|}\right)_0 e^{\alpha t}$

	cos θ range	$-t$ range	$\alpha(\text{GeV}/c)^{-2}$	$\left(\frac{d\sigma}{d t }\right)_0 \text{mb}/(\text{GeV}/c)^2$	Prob. (from χ^2)
Sol. I	0.98 - 0.20	0.046 - 1.329	3.81 ± 0.10	17.3 ± 1.7	0.05
Sol. II	0.98 - 0.70	0.046 - 0.686	4.29 ± 0.17	19.1 ± 2.0	0.08

TABLE III

Parameters for the fit of the form $\frac{d\sigma}{d|t|} = \left(\frac{d\sigma}{d|t|}\right)_0 e^{\alpha t + \beta t^2}$

	cos θ range	-t range	$\alpha(\text{GeV}/c)^{-2}$	$\beta(\text{GeV}/c)^{-4}$	$\left(\frac{d\sigma}{d t }\right)_0$ mb/(GeV/c) ²	Prob. (from χ^2)
Sol. I	0.98 - 0.20	0.046-1.829	4.64 \pm 0.25	0.74 \pm .20	19.7 \pm 2.0	0.20
Sol. II	0.98 - 0.50	0.046-1.143	4.55 \pm 0.39	0.64 \pm .42	19.5 \pm 2.3	0.15

Figure Captions

Fig. 1 The missing mass squared distribution for the events $K^+p \rightarrow Kp +$ Neutrals. The darkened area corresponds to events fitting and identified as $K^+p \rightarrow K^+\pi^0$.

Fig. 2 The experimental χ^2 distribution for a sample of 1450 elastic scattering events is shown, together with the expected distribution, for four-constraint type events. The experimental distribution has the correct shape, but is a factor 1.3 too narrow, indicating that the errors have been over-estimated by a factor 1.14 (a fact which has been observed in other experiments using the same chamber and measuring and computing system).

Fig. 3 The distribution of the dip angle, λ (defined as the angle between the plane of the chamber window and the scattering plane), for three intervals of the cosine of the scattering angle, θ .

- (a) For events in which $-1.0 \leq \cos \theta \leq 0.90$;
- (b) $0.90 \leq \cos \theta \leq 0.95$; and
- (c) $0.95 \leq \cos \theta \leq 0.98$.

The chosen cut-offs for each distribution are shown by the arrow and hatched area.

Fig. 4 The momentum dependence of the K^+p total cross-section (taken from References (2), (7), (8) and (11), and of the elastic cross-section (from References (1), (2), (3), (7) and this work), is given, for incident K^+ momenta up to 15 GeV/c.

Fig. 5 The corrected differential cross-section for K^+p scattering at 3.0 GeV/c is given as a function of momentum transfer squared, and of the cosine of the scattering angle. The curve is the best fit to the data of $\frac{d\sigma}{d|t|} = \left(\frac{d\sigma}{d|t|}\right)_0 e^{\alpha t + \beta t^2}$, with $\alpha = 4.64 \pm 0.25$ (GeV/c)⁻² and $\beta = 0.74 \pm 0.20$ (GeV/c)⁻⁴.

Fig. 6 The experimental angular distribution for K^+p elastic scattering is compared with two theoretical predictions. The curve (a) is an optical model prediction in which :

$$\frac{d\sigma}{d\Omega} = \left(\frac{d\sigma}{d\Omega}\right)_0 \left[\frac{P_L^1(\cos \theta) + P_{L+1}^1(\cos \theta)}{(L+1)^2} \right]^2,$$

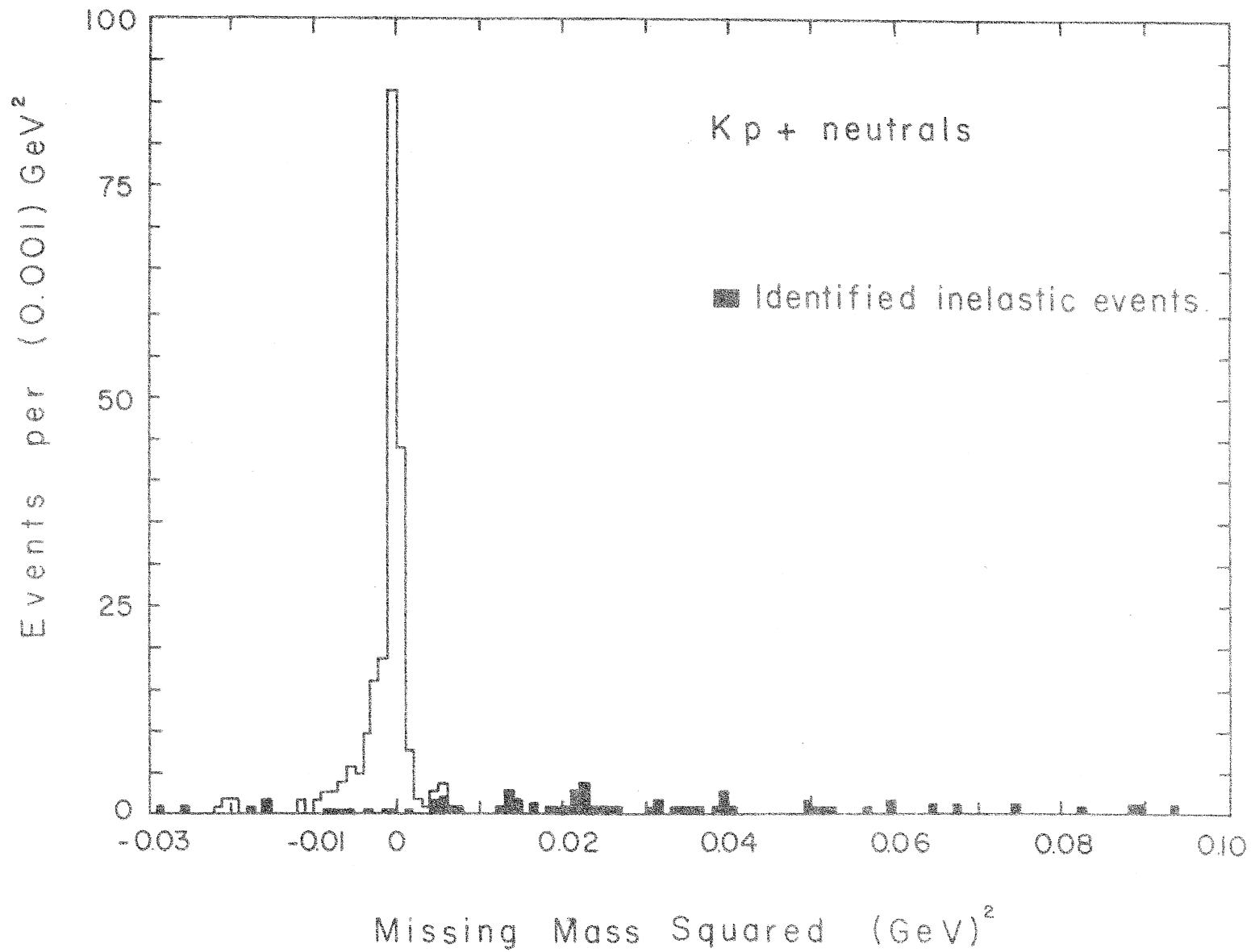
and with $L = 3$. The curve (b) is the best fit using the Minami formulation,

$$\frac{d\sigma}{d|t|} = e^{A_0 + A_1 t} + 2C e^{1/2(A_0 + A_1)t} + C^2.$$

The coefficients A_0 and A_1 are taken from Minami's analysis of the higher energy K^+p data (viz. $A_0 = 2.90$ and $A_1 = 5.6 \text{ (GeV/c)}^{-2}$), while C was varied to give best fit. C was found to be 0.4.

25283

Fig 1



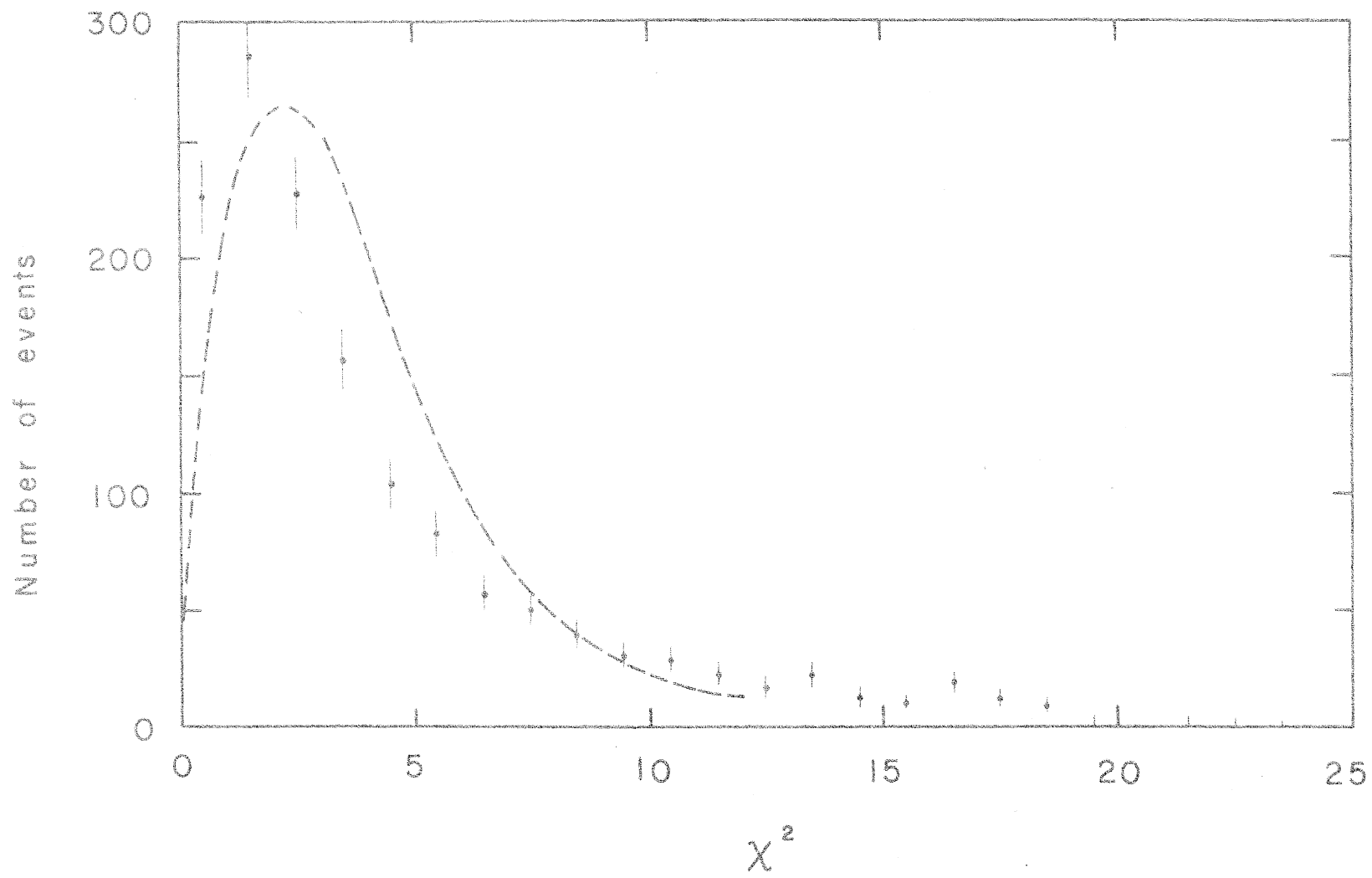
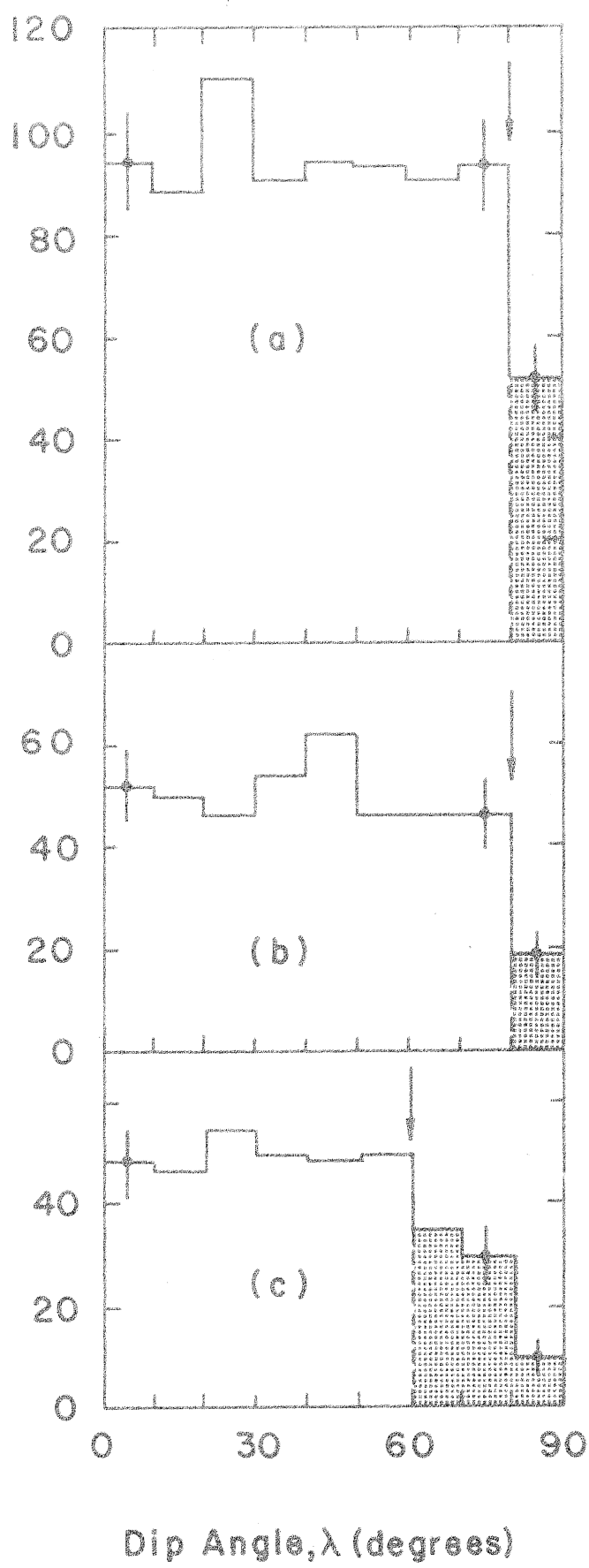


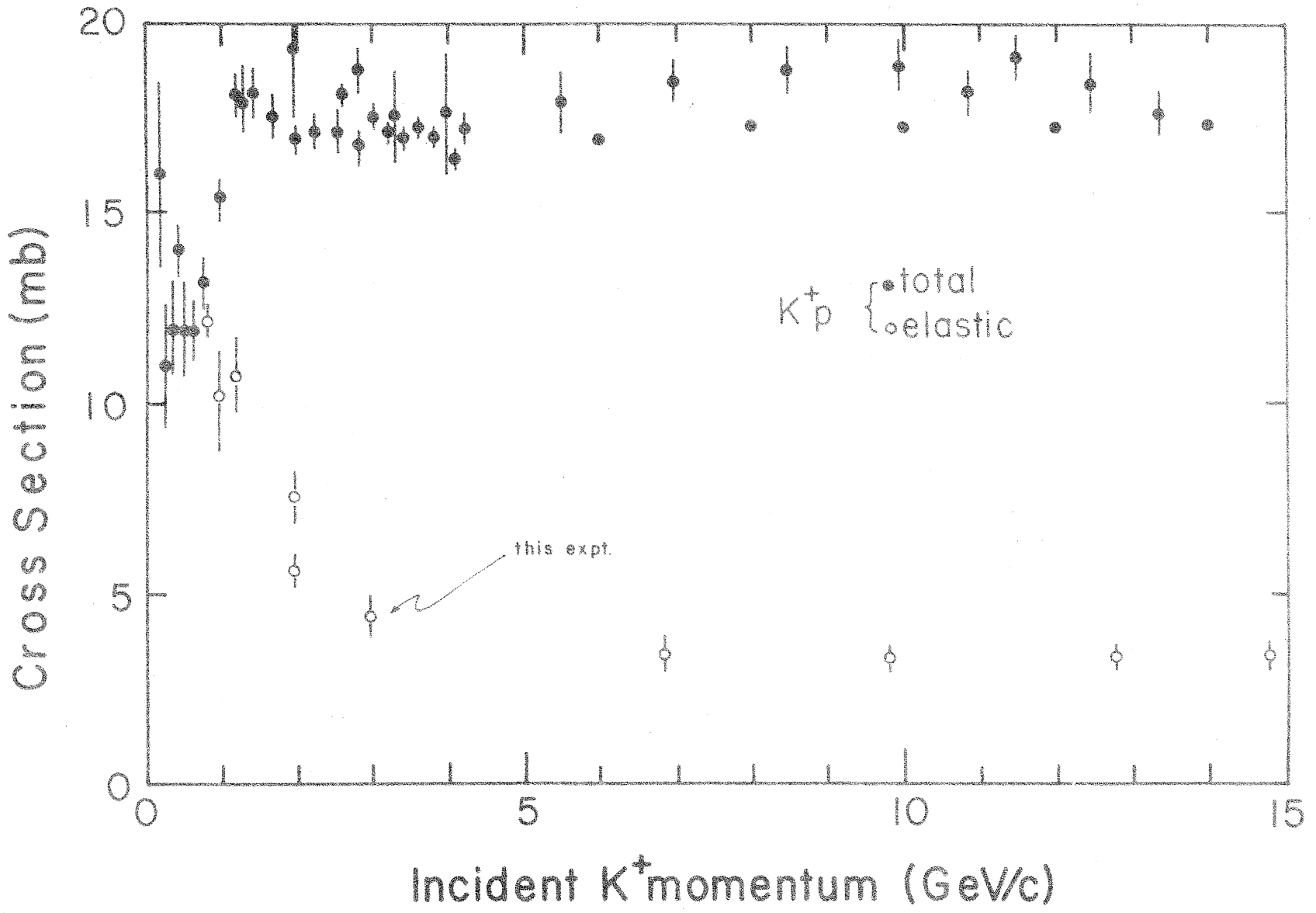
Fig 2

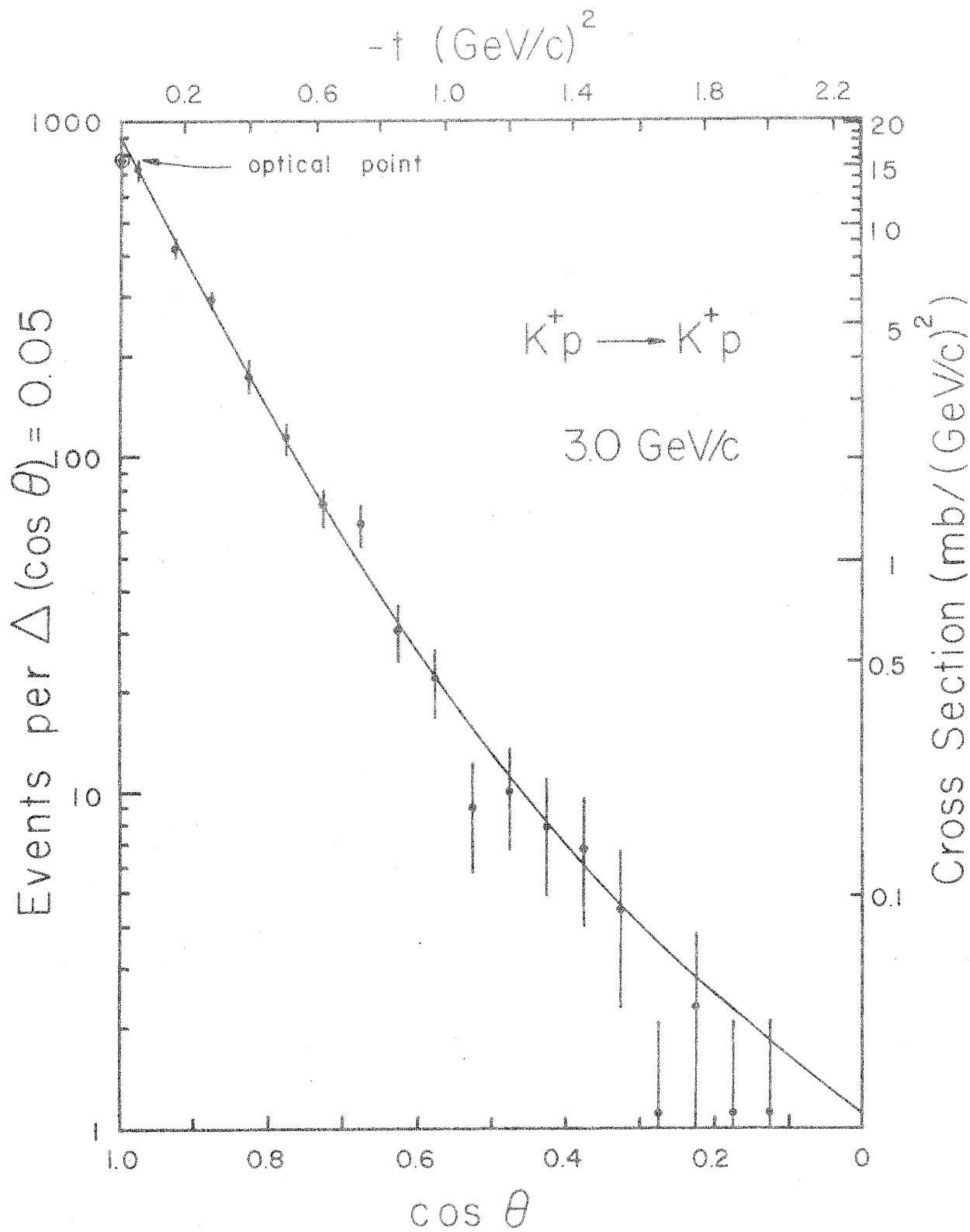
DIA 25288

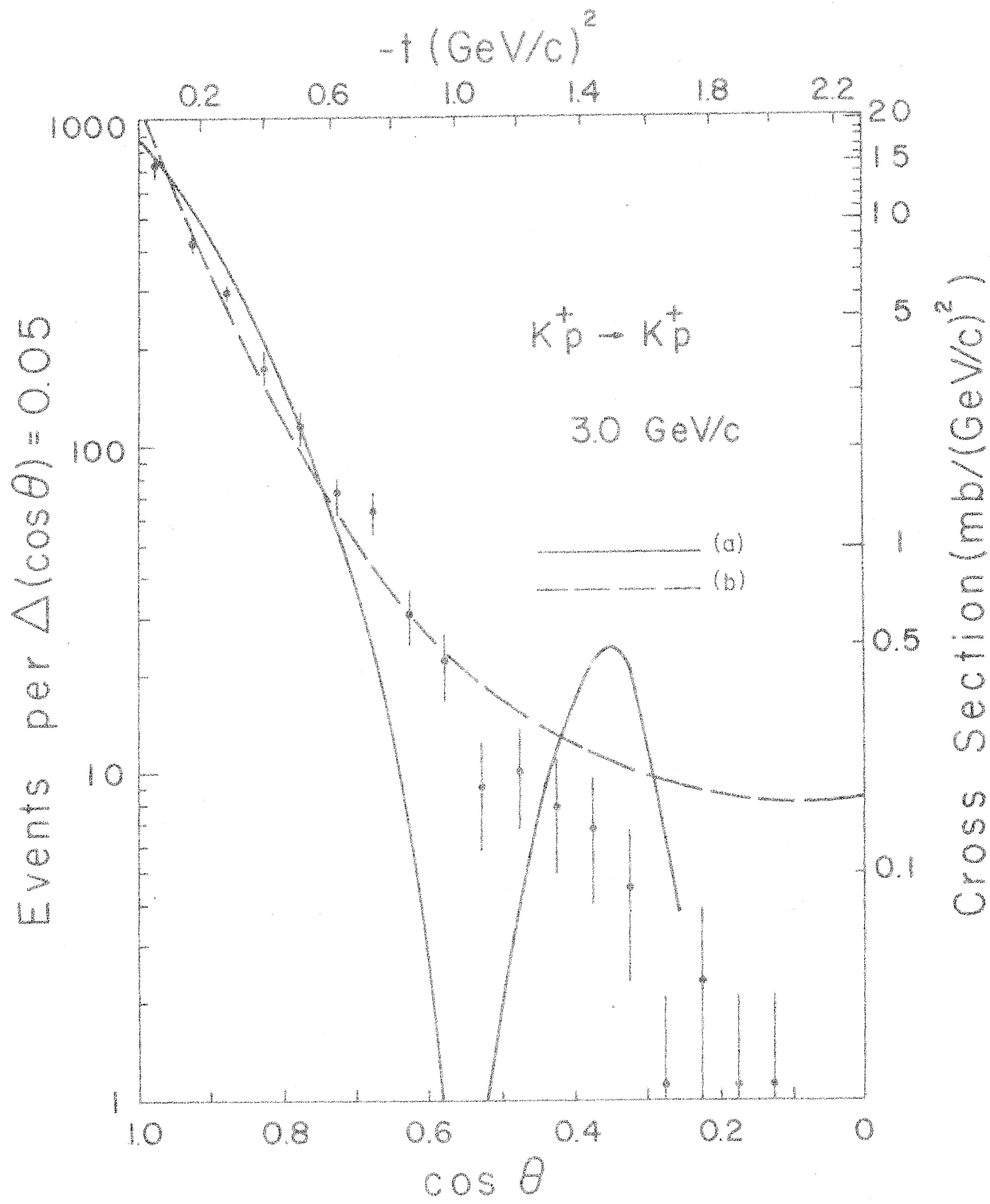
Number of events per 10-degree interval



DIA 25284 Fig. 4.







DIA 25285

Fig 6